

Volume 1  
Number 3

July 30, 1962

# Inorganic Chemistry

© Copyright 1962 by the American Chemical Society

CONTRIBUTION FROM THE INSTITUTE FOR ATOMIC RESEARCH AND  
DEPARTMENT OF CHEMISTRY, IOWA STATE UNIVERSITY, AMES, IOWA

## Ligand Field Theory of Square-Planar Platinum(II) Complexes<sup>1a</sup>

By RICHARD F. FENSKE, DON S. MARTIN, JR., AND KLAUS RUEDENBERG<sup>1b</sup>

Received January 13, 1962

The energy spectrum resulting from the  $5d^8$  configuration in a square-planar ligand field is calculated, using the point-dipole approximation, on the basis of a complete inner-configurational interaction, including spin-orbit coupling. The transition energies calculated for nine Pt(II) complexes are in good agreement with the observed spectra. The ordering of the d-orbitals is found to be as follows:  $d_{xz} = d_{yz} < d_{z^2} < d_{xy} < d_{x^2-y^2}$ . The disagreement between this result and a previous proposal is discussed in detail. Tables for the weak-field and strong-field basis functions and matrix elements are given.

### Introduction

In the past decade, the use of ligand field theory to explain the physical properties of the transition metal, rare earth, and actinide complexes has received wide interest; and it has been possible to understand characteristic variations in magnetic susceptibility, stability, ionic radii, and absorption spectra by application of this theory.<sup>2</sup>

Historically, ligand field theory makes the simplifying assumption that the effect of the symmetric ligands on the energy levels of the central ion in a complex can be explained by considering the ligands as point charges or point dipoles. The electrostatic interactions between these point charges or dipoles and the electrons cause a splitting of the originally degenerate d-orbitals in the case of the transition metal ions. The type of splitting is dependent upon the symmetry ar-

angement of the ligands. The degree of splitting is dependent upon the intensity of the electrostatic interaction.

To some extent, emphasis has been placed on the study of octahedral complexes of the first transition series. Not only is octahedral symmetry frequently encountered in complexes of interest, but it has the advantage that the ligand field potential can be expressed in terms of a single parameter,  $Dq$ . As Liehr<sup>3</sup> has pointed out, one can either interpret  $Dq$  in terms of electrostatic interactions or view it merely as a semi-empirical parameter in a molecular orbital calculation, which serves to assess the symmetry-induced separations of the d-orbitals.

In square-planar, as well as in tetragonal symmetry, the induced separations require three parameters, frequently denoted by  $Dq$ ,  $Ds$ , and  $Dt$ ,<sup>2,3</sup> if the argument is based on symmetry alone without specification of the source of the ligand field potential. If, however, the point charge or dipole model is introduced, reduction to two parameters is possible in the square-planar situation. These usually are specified as the "effective point charge" (or dipole) and the "ef-

(1) (a) Contribution No. 1021. This report is based on a Ph.D. thesis by Richard F. Fenske submitted April 1, 1961, to Iowa State University, Ames, Iowa. This work was performed partly under contract with the Atomic Energy Commission and partly under the support of a National Science Foundation Cooperative Fellowship for R.F.F. Presented at the Symposium on Ligand Field Theory, Division of Inorganic Chemistry, 140th National Meeting of the American Chemical Society, Chicago, Illinois, on September 7, 1961; (b) supported in part by a grant from the National Science Foundation.

(2) W. Moffitt and C. J. Ballhausen, *Ann. Rev. Phys. Chem.*, **7**, 107 (1956).

(3) A. D. Liehr, *J. Phys. Chem.*, **64**, 43 (1960).

fective radial distance."<sup>4</sup> The question has arisen<sup>3</sup> whether or not the point charge or dipole model is applicable to complexes of metallic ions in the fifth and sixth rows of the periodic table. Certain platinum(II) complexes seem well suited to test this approach.

The present work is concerned with the square-planar, diamagnetic complexes of platinum(II), such as  $[\text{PtCl}_4]^{-2}$ . While it may be argued that in solution such complexes actually are tetragonal, with solvent molecules occupying positions along the  $z$ -axis, the changes in the absorption spectra of such complexes in various solvents are, in fact, very slight.<sup>5</sup> This indicates that the energy levels are hardly affected by solvent interactions and, indeed, offer excellent illustrations of square-planar arrangements of the ligands about the central ion.

Further incentive to carry out the theoretical calculations for platinum(II) complexes was provided by a tentative interpretation, given by Chatt, Gamlen, and Orgel,<sup>6</sup> of the absorption spectra of  $[\text{PtCl}_4]^{-2}$  and ammonia-substituted chloroplatinates(II) in both solution and solid phases. Conveniently, these same absorption spectra were available to this Laboratory, as a result of previous interests in platinum complexes. Chatt, *et al.*,<sup>6</sup> proposed an energy level assignment which placed the  $d$ -orbitals of platinum(II) in the following order:  $d_{z^2} < d_{yz} = d_{xz} < d_{xy} < d_{x^2-y^2}$ .

Compared with similar assignments for square-planar symmetry in Ni(II) complexes,<sup>4b</sup> the proposals of Chatt, *et al.*,<sup>6</sup> differ in the relative placement of the degenerate  $d_{xz}$ ,  $d_{yz}$  orbitals and the  $d_{z^2}$  orbital. Since their assignment was based primarily on chemical evidence and some doubt concerning the validity of the assignment was expressed by the authors themselves, it was felt that a theoretical calculation, taking into account inner configurational interaction, might prove informative. Maki<sup>4b</sup> and Liehr and Ballhausen<sup>7</sup> have illustrated the necessity of including configuration interaction in calculations of the energy levels of Ni(II) complexes. Such considerations should be even more important in platinum complexes.

In their explanation of the platinum(II) absorption spectra, Chatt, *et al.*,<sup>6</sup> assigned certain

absorption maxima as due to singlet-to-triplet transitions. To justify the probability of such transitions they relied upon the appreciable spin-orbit coupling in platinum. It was felt that the inclusion of this effect in the configuration interaction calculations was another facet of the problem which made it worthwhile.

## 1. The $d^8$ Configuration in a Square-Planar Ligand Field

**General Considerations.**—The theoretical techniques applicable to the problem are well known.<sup>3,4,7</sup> The determination of the energy levels of the central ion requires the solution of Schrodinger's equation

$$\mathcal{H}\Psi = E\Psi \quad (1)$$

where

$$\mathcal{H} = \sum_i \{ -(\hbar^2/2m)\nabla_i^2 - (Ze^2/r_i) + \xi(r_i)(\vec{l}_i \cdot \vec{s}_i) \} + \sum_{i>j} (e^2/r_{ij}) + \sum_i V^{\text{LF}}(r_i)$$

The first four terms in the Hamiltonian,  $\mathcal{H}$ , are the usual atomic Hamiltonian operator for the free ion; in the last term,  $V^{\text{LF}}$ , expresses the effects of the non-spherical potential field of the surrounding ligands on an electron of the central ion.

The basic assumption of ligand field theory, as applied in this work, is that the field potential perturbs the atomic levels only in such a way as to modify the mixing of the wave functions belonging to one configuration. This means that one proceeds in a fashion analogous to the free ion problem.<sup>8</sup> In essence, the method reduces to the construction of matrices whose elements are given by

$$H'_{nm} = \langle \Psi_n | \mathcal{H}' | \Psi_m \rangle \quad (2)$$

where

$$\mathcal{H}' = \sum_{i>j} (e^2/r_{ij}) + \sum_i \xi(r_i)(\vec{l}_i \cdot \vec{s}_i) + \sum_i V^{\text{LF}}(r_i)$$

the sum being over only those electrons outside of filled subshells.

The first term in the Hamiltonian,  $\mathcal{H}'$ , concerns the coulombic interaction between the electrons, and in the case of the  $d_8$  configuration results in matrix elements which are functions of the two Slater-Condor<sup>8</sup> parameters,  $F_2$  and  $F_4$ . The second term accounts for the spin-orbit coupling and contributes matrix elements which most con-

(4) (a) C. J. Ballhausen, *Kgl. Danske Videnskab. Selskab, Mat.-fys. Medd.*, **29**, No. 4 (1955); (b) G. Maki, *J. Chem. Phys.*, **28**, 651 (1958).

(5) R. G. Pearson, H. B. Gray, and F. Basolo, *J. Am. Chem. Soc.*, **82**, 787 (1960).

(6) J. Chatt, G. A. Gamlen, and L. E. Orgel, *J. Chem. Soc.*, 486 (1958).

(7) A. D. Liehr and C. J. Ballhausen, *Ann. Phys.*, **6**, 134 (1959).

(8) E. U. Condon and G. H. Shortley, "The Theory of Atomic Spectra," Cambridge University Press, London, 1959.

veniently are expressed in terms of a parameter,  $\alpha = (1/2)\xi$ , where  $\xi$  is the Condon and Shortley<sup>8</sup> spin-orbit coupling constant. The final term is the contribution from the potential field of the ligands. For the point charge model, in square-planar symmetry, the potential,  $V^{LF}$ , has the form

$$V^{LF} = -q\{-4\sqrt{\pi}/\sqrt{5}R_2Y(2,0) + \sqrt{\pi}R_4Y(4,0) + (\sqrt{35}\pi/3\sqrt{2})R_4[Y(4,4) + Y(4,-4)]\} \quad (3)$$

where

$q$  = the effective ligand point charge

$R_1 = r_{<}/r_{>}^{l+1}$ ; with  $r_{>}$  = the greater, and  $r_{<}$  = the smaller of the two distances: (electron to central ion) and (ligand to central ion)

$Y(l,m) = Y_l^m(\theta,\Phi)$ , the normalized spherical harmonics<sup>9</sup> around the central ion

To obtain the point-dipole potential one differentiates the expression in eq. 3 with respect to the radial position coordinates of the ligands and replaces  $-q$  by  $\mu$ , where  $\mu$  is the effective point dipole.

The point-dipole ligand field contributes matrix elements which depend on two radial integrals,  $B_2$  and  $B_4$ , involving the atomic orbitals of the central ion. In this work, Slater orbitals<sup>9</sup> are used to evaluate these integrals, which then assume the form

$$B_1 = (4/315)\mu f \frac{d}{dx} G_1(x) \quad (4)$$

where

$\mu$  = the effective point dipole

$f = Z^*/n^*$  = Slater's effective nuclear charge/effective quantum number

$$G_1(x) = x^{-(l+1)} \int_0^x t^l e^{-2t} dt + x^l \int_x^\infty t^{-(l+1)} e^{-2t} dt$$

$x = fR$ , where  $R$  = the effective radial distance of the ligand

The wave functions,  $\Psi_n$  and  $\Psi_m$ , for the construction of the matrix elements are linear combinations of antisymmetrized products of one-electron functions. Two approaches can be used for choosing these basis functions, the *weak-field formulation* and the *strong-field formulation*.

**Weak-Field Formulation.**—Here the ligand field effect is presumed to be smaller than the electronic interaction effect. In this situation, a convenient basis set is obtained as follows.

If the ligand field potential is absent, the Hamiltonian in eq. 1 becomes that of the free ion. In this case, the nine energy levels of the  $d^8$  configuration have 45 state functions which are certain *linear combinations* of the wave functions associated with the terms:  ${}^3F_4$ ,  ${}^3F_3$ ,  ${}^3F_2$ ,  ${}^3P_2$ ,  ${}^3P_1$ ,

${}^3P_0$ ,  ${}^1G_4$ ,  ${}^1D_2$ , and  ${}^1S_0$ , where mixing of these takes place only among those terms which have the same  $J$  (total angular momentum) value. The 45 wave functions associated with these terms are characterized by  $|S,L,J,M_J\rangle$  where  $S$  = total spin momentum;  $L$  = total orbital angular momentum;  $J$  = total angular momentum;  $M_J$  =  $z$ -component of the total angular momentum.

With the inclusion of the ligand field potential, one no longer has spherical symmetry and the irreducible representations of the full rotation group now are reducible. Each term with a given  $J$  has a definite reduction into irreducible spin-space representations of the  $D_{4h}$  group. These reductions are given in Table I, in which Bethe's notation<sup>10</sup> for the irreducible representations is used.

TABLE I

IRREDUCIBLE REPRESENTATIONS OF  $J$  STATES IN  $D_4$ 

$J$ state	Irreducible representations <sup>a</sup>
0	$\Gamma_1$
1	$\Gamma_2 + \Gamma_5$
2	$\Gamma_1 + \Gamma_3 + \Gamma_4 + \Gamma_5$
3	$\Gamma_2 + \Gamma_3 + \Gamma_4 + \Gamma_5 + \Gamma_6$
4	$\Gamma_1 + \Gamma_1 + \Gamma_2 + \Gamma_3 + \Gamma_4 + \Gamma_5 + \Gamma_6$

<sup>a</sup> The notation for the irreducible representations is that due to Bethe.<sup>10</sup> The relation to the Mulliken notation is given in Table III.

Under the influence of the ligand field potential, those wave functions mix which are bases for the same irreducible representation. For example, as seen from Table I, in the  $\Gamma_2$  irreducible representation, the mixing will take place between certain functions arising from the  ${}^1G_4$ ,  ${}^3F_4$ ,  ${}^3F_3$ , and  ${}^3P_1$  terms. In terms of the  $|S,L,J,M_J\rangle$  functions, the symmetry-adapted basis functions for this representation are

$$\begin{aligned} & \text{in } ({}^1G_4): (1/i\sqrt{2})\{|0, 4, 4, 4\rangle - |0, 4, 4, -4\rangle\} \\ & \text{in } ({}^3F_4): (1/i\sqrt{2})\{|1, 3, 4, 4\rangle - |1, 3, 4, -4\rangle\} \\ & \text{in } ({}^3F_3): |1, 3, 3, 0\rangle \\ & \text{in } ({}^3P_1): |1, 1, 1, 0\rangle \end{aligned}$$

Consequently, by suitable linear combinations of the  $|S,L,J,M_J\rangle$  functions as illustrated above, there occurs a factorization of the  $45 \times 45$  matrix into five sub-blocks corresponding to the five irreducible representations of the  $D_{4h}$  group. Since  $\Gamma_5$  is doubly degenerate, it further decomposes into two identical sub-blocks. The  $\Gamma_2$  case just mentioned obviously is a  $4 \times 4$  matrix prob-

(9) I. C. Slater, *Phys. Rev.*, **36**, 57 (1930).(10) H. Bethe, *Ann. Physik*, **3**, 133 (1929).

lem. The others are:  $\Gamma_1$ :  $9 \times 9$ ;  $\Gamma_3$ :  $6 \times 6$ ;  $\Gamma_4$ :  $6 \times 6$ ;  $\Gamma_5$ :  $10 \times 10$ .

The choice of basis functions just outlined yields energy matrices which are diagonal in the electronic interaction terms, because the basis functions are linear combinations of the free ion terms under  $L$ - $S$  coupling. The ligand field and spin-orbit coupling terms contribute both diagonal and off-diagonal elements. The complete matrices for the weak field approach to the  $d^8$  configuration in  $D_4$  symmetry have not been given before and therefore are included in the Appendix.

In the weak-field *approximation*, the off-diagonal elements are ignored. Here, however, the  $45 \times 45$  eigenvalue problem is solved exactly.

**Strong-Field Formulation.**—In this case, the ligand field effect is considered to be greater than the electronic interaction and the spin-orbit coupling. Consider, therefore, the Hamiltonian of eq. 1 in the instance where the latter two effects are neglected. Then the matrix,  $H'_{nm}$ , of eq. 2 will be diagonal if the  $\Psi_n$  are chosen as bases for the irreducible representations of the symmetry group of the ligands. Such bases are most easily constructed as antisymmetric products of one-electron functions which themselves are symmetry adapted. Since it is convenient that the final functions be symmetry adapted with respect to both spin and space coordinates, the spin functions, also, are taken in such linear combinations as to be basis functions in spin or space for the irreducible representations of the group of the ligands. For the two-electron case at hand,<sup>11</sup> the strong-field basis functions can be formed as follows.

Construct symmetry-adapted one-electron functions from linear combinations of the  $|l, m_l\rangle$  functions. For the transition metals, they are the familiar functions:  $d_{x^2-y^2}$  (spanning  $\Gamma_3$ ),  $d_{z^2}$  (spanning  $\Gamma_1$ ),  $d_{xy}$  (spanning  $\Gamma_4$ ), and  $d_{xz}$ ,  $d_{yz}$  (spanning  $\Gamma_5$ ). Next, construct two-electron symmetry-adapted functions by taking certain linear combinations of all possible products of these one-electron functions. These are easily chosen as to be either symmetric or antisymmetric in the two electrons. The representation of a particular product function is obtained by the direct product theorem of group theory.

Now construct symmetry-adapted spin func-

(11) By means of the "electron hole" formalism, the  $d^8$  configuration is handled as if it were  $d^2$ . Only the signs ( $\pm$ ) of the  $L$ - $S$  coupling and ligand field matrix elements need be changed (see Appendix).

tions. In  $D_4$ , the singlet function belongs to the representation  $\Gamma_1$ , whereas the triplet decomposes into  $\Gamma_2 + \Gamma_5$ , where  $\Gamma_3$  is spanned by  $\alpha(1)\alpha(2)$  and  $\beta(1)\beta(2)$ .

The final symmetry-adapted basis functions are obtained as those reduced direct products between the space basis and the spin basis which yield totally antisymmetric functions in the electrons. The representations of the final functions again are determined by the direct product theorem.

The final functions will factor the  $45 \times 45$  matrix into sub-blocks corresponding to the irreducible representations of the group, just as did the functions given in the weak-field approach. Moreover, the size of each sub-block is identical in the two cases. This arises from the fact that the basis functions of the weak- and strong-field formulations are connected by a unitary transformation which itself factors into six subtransformations, each of which operates only within the subspace of a given irreducible representation. Whereas in the weak-field formulation the matrix elements are diagonal in the electronic interaction terms, in the strong-field approach each of the matrices is diagonal in the ligand field parameters, with the electronic interaction and spin-orbit coupling terms contributing to diagonal and off-diagonal elements. The strong-field matrix elements, which also have not been listed so far, are given in the Appendix.

In the strong-field *approximation*, the off-diagonal elements are ignored; in this work, however, the complete diagonalization is carried out. In view of the unitary connection mentioned above, the eigenvalues must be identical with those of the weak-field diagonalization. This served as a convenient check for the computations.

## 2. Calculation of Energy Levels

**Assumptions.**—Values for the five parameters,  $F_2$ ,  $F_4$ ,  $\alpha$ ,  $R$ , and  $\mu$ , were chosen from the following considerations.

(1) In atomic theory,<sup>8</sup> it is shown that the two Slater-Condon parameters are approximately related by the equation

$$F_2 = 14F_4$$

(2) By use of the above relation and a knowledge of the theoretical and experimental values of the energy levels in the free ion,  $Pt^{+1}$ , an estimate of the  $F_4$  parameter was determined to be  $3.92 \times 10^{-4}$  atomic unit. It was necessary to

estimate  $F_2$  and  $F_4$  in this fashion since the experimental energy levels of the free ion,  $\text{Pt}^{+2}$ , are not available at the present time.

(3) The final value for the spin-orbit coupling parameter,  $\alpha$ , for platinum was that given by McClure,<sup>12</sup> namely,  $9.42 \times 10^{-2}$  atomic unit. However, initial calculations also were made with  $\alpha = 0$ , since under this condition there is a clear separation between the singlet and triplet states.

(4) For the majority of the complexes, the final value for the effective radial distance,  $R$ , was chosen to be 2.34 Å. (4.5 atomic units), which is the internuclear distance between the platinum and chlorine atoms in solid  $\text{K}_2\text{PtCl}_4$  as given by X-ray diffraction data.<sup>13</sup> Because certain authors have obtained better agreement by use of a radial distance somewhat less than the internuclear distance, some of the initial calculations were carried out with  $R$  equal to 2.2 Å. This latter value, which corresponds to the platinum-to-ammonia distance in mixed complexes,<sup>14</sup> also was used to obtain improved agreement between theory and experiment for *cis*- $[\text{Pt}(\text{NH}_3)_2\text{Cl}_2]$  and  $[\text{Pt}(\text{NH}_3)_3\text{Cl}]^{+1}$ .

(5) Energy levels then were calculated as functions of  $\mu$ , the effective dipole moment of the ligands. As will be discussed later, the appropriate value of this parameter for a given complex then was fixed by reference to one specific absorption maximum.

(6) In actuality, the effects of changes in all the parameters on the energy levels were investigated, but in the final analysis the foregoing not only were justified by the considerations mentioned but, as indicated in Section 3, gave the best agreement with experiment.

**Results.**—For the chosen values of the five parameters, diagonalization of the weak and strong-field matrices by means of the Iowa State Cyclone digital computer gave eigenvalues which agreed to seven significant figures. The only exception was the  $\Gamma_6$  representation with spin-orbit coupling where agreement existed to only five figures. The inclusion of spin-orbit coupling leads to a complex matrix whose diagonalization is equivalent to that of a real matrix twice as large; in the case of  $\Gamma_6$ , it has the dimension  $20 \times 20$ .

As a typical example of the results obtained, Fig. 1 illustrates the effects of increasing dipole moment on the energy levels of the  $d^8$  configura-

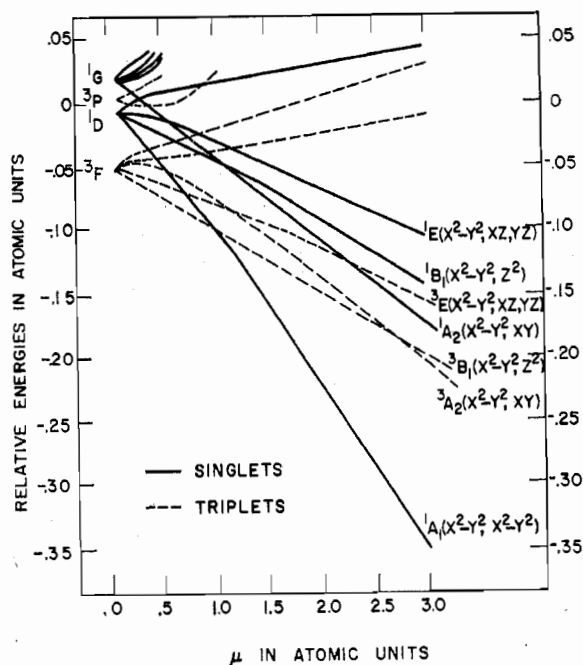


Fig. 1.—Energy levels of Pt(II) as a function of the effective dipole moment of the ligands. Parameter values:  $\alpha = 0$ ,  $F_2 = 0.005488$  a.u.,  $F_4 = 0.000392$  a.u.,  $R = 4.23$  a.u. (2.20 Å.). The symmetry labels characterize the spatial part of the wave functions. The orbitals in parentheses are those vacant in the strong-field approximation.

tion in square-planar symmetry. This particular calculation assumes no spin-orbit coupling. Hence, singlets and triplets do not mix and the symmetry labels,  $A_1$ ,  $B_1$ ,  $A_2$ , and  $E$ , characterize the spatial portions of the wave functions. The orbitals listed in parentheses on the right hand side of the figure correspond to the vacant orbitals for the particular state in the strong field approximation. Because of configuration interaction, such assignments are not strictly valid, but for  $\mu$  values in excess of two atomic units, the wave functions associated with the states are principally those indicated.

If one considers that the primary effect of spin-orbit coupling is to increase the probability of singlet-to-triplet transitions, certain characteristics are evident from the figure.

Since the ground state of the free ion is a triplet state, it exhibits paramagnetic behavior. However, a complex whose effective ligand dipole moment is greater than 1.0 atomic unit will be diamagnetic. This is the case for all known Pt(II) complexes. In the ground state, electrons occupy all the orbitals except the  $d_{x^2-y^2}$  orbital and hence the absorption maxima are due to electron transitions from the filled orbitals to this vacant one.

(12) D. S. McClure, *Solid State Phys.*, **9**, 399 (1959).

(13) R. G. Dickinson, *J. Am. Chem. Soc.*, **44**, 2404 (1920).

(14) M. Atoji, J. W. Richardson, and R. E. Rundle, *ibid.*, **79**, 3017 (1957).

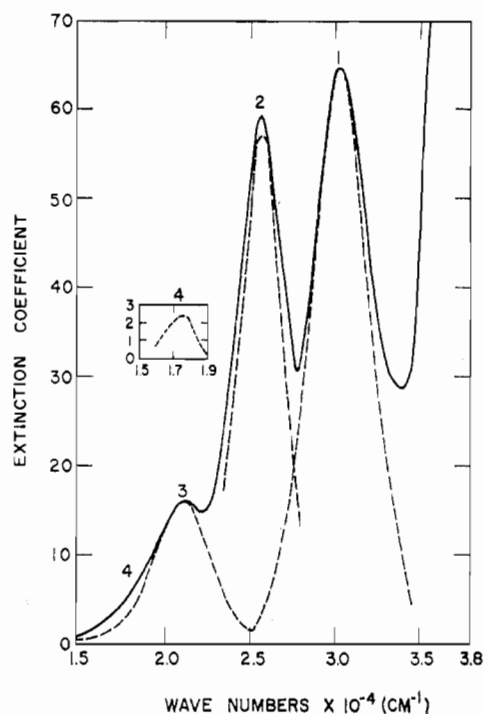


Fig. 2.—Gaussian analysis of the absorption spectrum of aqueous  $\text{PtCl}_4^{-2}$ .

From the figure, it also is seen that for such diamagnetic complexes, the first excited singlet state results from the transfer of an electron from the  $d_{xy}$  to the  $d_{x^2-y^2}$  orbital, and the next excited singlet state results from the electron jump:  $d_{z^2} \rightarrow d_{x^2-y^2}$ .

The latter conclusion is in contradiction to the interpretation suggested by Chatt, *et al.*,<sup>6</sup> namely that the transition corresponds to  $d_{xz}, d_{yz} \rightarrow d_{x^2-y^2}$ . While Fig. 1 does not take spin-orbit coupling into account and the radial distance used is somewhat less than the final chosen value, these changes in the parameters do not alter the relative positions of the  $^1B_1$  and  $^1E$  states. This disagreement with the aforementioned authors concerning the ordering of the d-orbitals will be discussed more fully in Section 4.

### 3. Absorption Spectra of the Pt(II) Complexes

**Observed Spectra.**—Figure 2 illustrates the gaussian analysis of the absorption spectrum of  $[\text{PtCl}_4]^{-2}$  as carried out by Chatt, *et al.*,<sup>6</sup> and repeated independently for this work. The position of "peak 4" in the figure was hypothesized by Chatt, *et al.*,<sup>6</sup> strictly on the basis of the gaussian analysis. In fact, for a number of the complexes considered, the resolution of peaks 3 and 4 was

not achieved. In view of the low extinction coefficients and the uncertainty in the complete applicability of the gaussian analysis, it was held in this work that an accurate placement of two maxima could not be realized. Hence, peak 3 in each spectrum has been left as possibly an unresolved combination of two low-probability transitions.

The general characteristics of the spectrum in Fig. 2 are applicable to all the complexes considered. That is, the lowest energy maximum is of low intensity (peak 3), followed by two moderately intense absorption bands (peaks 2 and 1), and finally by an intense absorption band whose maximum appears, in this case, at a wave number beyond the range of the spectrophotometer. Because of its intensity, this latter peak was presumed by Chatt, *et al.*,<sup>6</sup> to be due to an electron transition from a d-orbital to a p-orbital, and therefore falls out of the range of the present treatment.

When ammonia or water molecules are substituted for one or more of the chloride ions in the complex, there is a systematic shift of the absorption maxima to shorter and shorter wave lengths. This suggests that despite some changes in intensity, the same d-to-d orbital transitions are involved in  $[\text{Pt}(\text{NH}_3)\text{Cl}_3]^{-1}$ , *cis*- and *trans*- $[\text{Pt}(\text{NH}_3)_2\text{Cl}_2]$ , etc., as take place in  $[\text{PtCl}_4]^{-2}$ , and one reasonably may assume that all may be treated as if they possessed square-planar symmetry. The absorption maxima corresponding to peaks 1, 2, and 3 for the complexes considered in this work are given in Table II.

**Theory and Experiment.**—If, as a first approximation, one considers the energy levels of Fig. 1 as indicative of the transitions involved, the region of high dipole moment,  $>2.5$  atomic units, suggests a ready interpretation of the observed spectra.

The lowest energy, low intensity band (peak 3) corresponds to two singlet-to-triplet transitions. This assignment is in keeping with the appreciable spin-orbit coupling present in platinum. The fact that the gaussian analyses of the spectra seem to indicate the presence of two peaks of similar energy correlates with the two-triplet energy levels, given in Fig. 1, which cross at 2.75 atomic units.

The first of the moderately intense bands (peak 2) then is in keeping with the singlet-to-singlet transition of an electron from the  $d_{xy}$  to the  $d_{x^2-y^2}$  orbital. This, as well as the previous singlet-

TABLE II  
 COMPARISON OF FINAL TRANSITION ENERGIES WITH OBSERVED SPECTRAL MAXIMA<sup>a</sup>

Compd. <sup>b</sup>	Peak 2 std. <sup>1</sup> A <sub>1</sub> → <sup>1</sup> A <sub>2</sub>	Dipole moment (a.u.)	Peak 1		Peak 3		
			Obsd.	Calcd. A <sub>1</sub> → <sup>1</sup> B <sub>1</sub>	Obsd.	Calcd. <sup>1</sup> A <sub>1</sub> → <sup>3</sup> A <sub>2</sub>	Calcd. <sup>1</sup> A <sub>1</sub> → <sup>3</sup> B <sub>1</sub>
First calculation <sup>c</sup>							
1	2.55	2.89	3.02	2.92	2.10	2.20	2.16
2	2.89	3.24	3.33	3.28	2.41	2.48	2.50
3	3.17	3.38	3.67	3.61	2.68	2.74	2.83
4	3.12	3.34	3.71	3.53	2.64	2.70	2.76
5	3.33	3.51	3.72	3.81	2.73	2.76	3.00
6	2.64	2.96	3.14	3.02	<sup>d</sup>	2.28	2.26
7	2.72	3.02	3.18	3.11	<sup>d</sup>	2.34	2.34
8	2.90	3.16	3.33	3.31	<sup>d</sup>	2.51	2.51
9	3.60	3.70	3.92	4.10	3.10	3.10	3.25
Second calculation <sup>e</sup>							
5	3.33	2.74	3.72	3.68	2.73	2.90	2.80
9	3.60	2.92	3.92	3.99	3.10	3.10	3.16

<sup>a</sup> All results are in wave numbers  $\times 10^{-4}$  (cm.<sup>-1</sup>). <sup>b</sup> The complexes are: 1, [PtCl<sub>4</sub>]<sup>-2</sup>; 2, [Pt(NH<sub>3</sub>)Cl<sub>3</sub>]<sup>-1</sup>; 3, *trans*-[Pt(NH<sub>3</sub>)<sub>2</sub>Cl<sub>2</sub>]; 4, *trans*-[Pt(*n*-C<sub>5</sub>H<sub>11</sub>)<sub>2</sub>NH]<sub>2</sub>Cl<sub>2</sub>]; 5, *cis*-[Pt(NH<sub>3</sub>)<sub>2</sub>Cl<sub>2</sub>]; 6, [Pt(H<sub>2</sub>O)Cl<sub>3</sub>]<sup>-1</sup>; 7, (Pt(OH)Cl<sub>3</sub>)<sup>-2</sup>; 8, [Pt(OH)<sub>2</sub>Cl<sub>2</sub>]<sup>-2</sup>; 9, [Pt(NH<sub>3</sub>)<sub>3</sub>Cl]<sup>+1</sup>. <sup>c</sup> Values of the parameters of Group I calculations are:  $R = 2.34$  Å.,  $F_2 = 0.005488$  a.u.,  $F_4 = 0.000392$  a.u.,  $\alpha = 0.00942$ . <sup>d</sup> Experimental values unknown. <sup>e</sup> Values of the parameters for Group II calculations are:  $R = 2.20$  Å.,  $F_2 = 0.005488$  a.u.,  $F_4 = 0.000392$  a.u.,  $\alpha = 0.00942$  a.u.

to-triplet assignment, is in accord with the transitions hypothesized by Chatt, *et al.*<sup>8</sup>

The other band of moderate intensity (peak 1) then is assignable as a singlet-to-singlet transition from the  $d_{x^2}$  to the  $d_{x^2-y^2}$  orbital. Any low-intensity transition to the triplet state lying between the <sup>1</sup>A<sub>1</sub> and <sup>1</sup>B<sub>1</sub> energy levels of Fig. 1 would be masked by the more preferred singlet-to-singlet transitions.

The foregoing assignment postulates that the singlet-to-singlet transition of an electron from the degenerate  $d_{xz}$ ,  $d_{yz}$  orbitals to the  $d_{x^2-y^2}$  orbital is hidden by the d-to-p transition previously mentioned.

There remains the task of justifying the assignment by correlation of experimental and predicted values of the absorption maxima. Figure 3 displays the pertinent transition energies as a function of  $\mu$  for the final values of  $F_2$ ,  $F_4$ ,  $\alpha$ , and  $R$ . For clarity, certain predominantly singlet-to-triplet transitions whose energies are comparable to the more likely singlet-to-singlet transitions have been omitted from the figure.

The effective dipole moment values for eight complexes were fixed by matching the theoretical <sup>1</sup>A<sub>1</sub> to <sup>1</sup>A<sub>2</sub> transitions to the values of peak 2. Table II compares the remaining transition energies for the complexes with the experimental absorption maxima. As indicated by the table and by Fig. 3, reasonable agreement is achieved.

It is gratifying that, for the ammino, aquo, and hydroxy complexes with the formulas (PtL<sub>*n*</sub>Cl<sub>4-*n*</sub>),

where L = (NH<sub>3</sub>), (H<sub>2</sub>O), or (OH)<sup>-</sup>, the dipole moments are given approximately by the expressions

$$\begin{aligned}\mu(\text{L}_n\text{Cl}_{4-n}) &= n\mu(\text{L}) + (4-n)\mu(\text{Cl}) \\ \mu(\text{Cl}) &= 0.7225 \text{ a.u.} \\ \mu(\text{H}_2\text{O}) &= 0.8125 \text{ a.u.} \\ \mu(\text{OH}^-) &= 0.8525 \text{ a.u.} \\ \mu(\text{NH}_3) &= 0.9725 \text{ a.u.}\end{aligned}$$

It may be noted that, in the cases of *cis*-[Pt(NH<sub>3</sub>)<sub>2</sub>Cl<sub>2</sub>] and [Pt(NH<sub>3</sub>)<sub>3</sub>Cl]<sup>+</sup>, an improvement resulted when the platinum-to-ammonia distance of 2.2 Å. was used for the radial distance parameter of the point-dipoles.

#### 4. Ordering of d-Orbitals in Pt(II)

I.—The foregoing results lead to the conclusion that in the strong field present in platinum(II) complexes, the d-orbitals fall into the order

$$d_{xz} = d_{yz} < d_{z^2} < d_{xy} < d_{x^2-y^2}$$

This result differs from the ordering suggested by Chatt, *et al.*,<sup>8</sup> in the relative positions of the  $d_{x^2}$  and the  $d_{xz}$ ,  $d_{yz}$  orbitals.

With one exception, all the features of the spectra used by Chatt, *et al.*,<sup>8</sup> to substantiate their assignment are equally compatible with the present alternative assignment. Without going into detail, this single feature concerns the absorption spectra of the *solid* complexes, and involves the conjecture that the levels in the solids are the same as those of the complexes in solution. This assumption would rest on reasonably firm ground



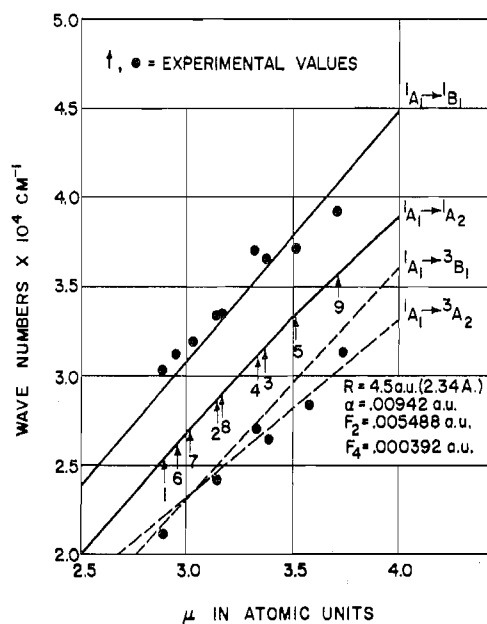


Fig. 3.—Transition energies as functions of dipole moment for the final choice of parameters. Because of spin-orbit coupling, the states involved in the transitions are *not exactly, but primarily*, those indicated at the right hand side. The experimental absorption peaks of a given complex lie in one vertical. The arrows indicate those experimental values whose fit to the theoretical curve determines the dipole moments for the various complexes. The latter are identified by the same numbers as are used in Table II.

if the absorption peaks in the two situations would be identical, as they are in certain Ni(II) complexes investigated by Maki.<sup>15</sup> Such is *not* the case, however, with the platinum complexes under discussion. For example, the three peaks in the solution spectrum of  $K_2PtCl_4$  are at 331, 392, and 476  $m\mu$ , while in the spectrum of the solid, the peaks are at 340, 375, and 500  $m\mu$ . While these are somewhat close, it should be noted that the shifts are in different directions.

Furthermore, Dickinson<sup>13</sup> has pointed out that in solid  $K_2PtCl_4$  the platinum atoms appear in

TABLE III  
SYMMETRY-ADAPTED 5d-ORBITALS FOR  $D_{4h}$  SYMMETRY

Representation Bethe Mulliken	5d-orbital	Notation used in Table VII to denote orbitals
$\Gamma_1$ $A_1$	$5d(z^2) \sim z^2 r e^{-fr}$	<i>a</i>
$\Gamma_3$ $B_1$	$5d(x^2 - y^2) \sim (x^2 - y^2) r e^{-fr}$	<i>b</i>
$\Gamma_4$ $B_2$	$5d(xy) \sim xy r e^{-fr}$	<i>c</i>
$\Gamma_5$ $E$	$5d(xz) \sim xz r e^{-fr}$	<i>d</i>
	$5d(yz) \sim yz r e^{-fr}$	<i>e</i>

(15) G. Maki, *J. Chem. Phys.*, **29**, 162 (1958).

TABLE IV  
THE LIGAND-FIELD INTEGRALS FOR  $D_{4h}$  SYMMETRY AND  
SQUARE-PLANAR DIPOLE MODEL

Parameter	Tetragonal symmetry	Square-planar point dipole model
$Q_2$	$Dq + 2Ds - Dt$	$(1/14)B_4 + (4/7)B_2$
$Q_1$	$-4Dq - Ds + 4Dt$	$-(2/7)B_4 - (2/7)B_2$
$Q_0$	$6Dq - 2Ds - 6Dt$	$(3/7)B_4 - (4/7)B_2$
$B_{2-2}$	$5Dq$	$(5/6)B_4$

TABLE V  
WEAK-FIELD BASIS FUNCTIONS

$\Gamma_1$ Representation	Triplets
Singlets	
(1) = $[^1G_4(4) + ^1G_4(-4)]/\sqrt{2}$	(3) = $[^3F_4(2) - ^3F_4(-2)]/i\sqrt{2}$
(2) = $^1G_4(0)$	(4) = $[^3F_3(2) + ^3F_3(-2)]/\sqrt{2}$
(3) = $^1D_2(0)$	(5) = $[^3F_2(2) - ^3F_2(-2)]/i\sqrt{2}$
(4) = $^1S_0(0)$	(6) = $[^3P_2(2) - ^3P_2(-2)]/i\sqrt{2}$
Triplets	
(5) = $[^3F_4(4) + ^3F_4(-4)]/\sqrt{2}$	
(6) = $^3F_4(0)$	
(7) = $^3F_2(0)$	
(8) = $^3P_2(0)$	
(9) = $^3P_0(0)$	
$\Gamma_3$ Representation	
Singlets	
(1) = $[^1G_4(4) - ^1G_4(-4)]/i\sqrt{2}$	(1) = $[^1G_4(-3) - ^1G_4(3)]/\sqrt{2}$
Triplets	
(2) = $[^3F_4(4) - ^3F_4(-4)]/i\sqrt{2}$	(2) = $[^1G_4(-1) - ^1G_4(1)]/\sqrt{2}$
(3) = $^3F_3(0)$	(3) = $[^1D_2(-1) - ^1D_2(1)]/\sqrt{2}$
(4) = $^3P_1(0)$	
$\Gamma_5$ Representation	
Singlets	
(1) = $[^1G_4(2) + ^1G_4(-2)]/\sqrt{2}$	(1) = $[^1G_4(-3) + ^1G_4(3)]/i\sqrt{2}$
(2) = $[^1D_2(2) + ^1D_2(-2)]/\sqrt{2}$	(2) = $[^1G_4(-1) + ^1G_4(1)]/i\sqrt{2}$
Triplets	
(3) = $[^3F_4(2) + ^3F_4(-2)]/\sqrt{2}$	(3) = $[^1D_2(-1) + ^1D_2(1)]/i\sqrt{2}$
(4) = $[^3F_3(2) - ^3F_3(-2)]/i\sqrt{2}$	
(5) = $[^3F_2(2) + ^3F_2(-2)]/\sqrt{2}$	
(6) = $[^3P_2(2) + ^3P_2(-2)]/\sqrt{2}$	
$\Gamma_4$ Representation	
Singlets	
(1) = $[^1G_4(2) - ^1G_4(-2)]/i\sqrt{2}$	(4) = $[^3F_4(-3) + ^3F_4(3)]/i\sqrt{2}$
(2) = $[^1D_2(2) - ^1D_2(-2)]/i\sqrt{2}$	(5) = $[^3F_3(-1) + ^3F_3(1)]/i\sqrt{2}$
	(6) = $[^3F_2(-1) + ^3F_2(1)]/i\sqrt{2}$
	(7) = $[^3P_2(-1) + ^3P_2(1)]/i\sqrt{2}$
	(8) = $[^3F_3(3) - ^3F_3(-3)]/\sqrt{2}$
	(9) = $[^3F_2(1) - ^3F_2(-1)]/\sqrt{2}$
	(10) = $[^3P_1(1) - ^3P_1(-1)]/\sqrt{2}$

chains one above another, whereas it is expected that in aqueous solution, water molecules would be oriented such that the negative ends of their dipoles are directed toward the platinum ion. In view of the fact that in certain crystals complex ions of platinum are known to form metal-metal bonds,<sup>14</sup> it is possible that related interactions may be present to some degree in solid  $K_2PtCl_4$ , so that there may be significant differences between its spectrum in the solid and in solution. In ligand field terms, the positive charges due to neighboring platinum ions could alter the positions of the energy levels.

A further assumption for the argument of Chatt, *et al.*,<sup>6</sup> to be conclusive is that the transitions are made vibrationally allowed by stretching



TABLE VI  
WEAK-FIELD MATRIX ELEMENTS

<p><math>\Gamma_1</math> Representation Singlet matrix</p> <p>(1) 1) = <math>2Q_2 + 4F_2 + F_4</math>            (2) 1) = <math>(2/\sqrt{35})B_{2-2}</math>            (2) 2) = <math>(2/35)(Q_2 + 16Q_1 + 18Q_0) + 4F_2 + F_4</math>            (3) 1) = <math>(4/\sqrt{7})B_{2-2}</math>            (3) 2) = <math>(4/7\sqrt{5})(Q_2 + 2Q_1 - 3Q_0)</math>            (3) 3) = <math>(2/7)(4Q_2 + Q_1 + 2Q_0) - 3F_2 + 36F_4</math>            (4) 1) = <math>(4/\sqrt{10})B_{2-2}</math>            (4) 2) = <math>(4/5\sqrt{14})(Q_2 - 4Q_1 + 3Q_0)</math>            (4) 3) = <math>(4/\sqrt{70})(2Q_2 - Q_1 - Q_0)</math>            (4) 4) = <math>(2/5)(2Q_2 + 2Q_1 + Q_0) + 14F_2 + 126F_4</math></p> <p>Triplet matrix</p> <p>(5) 5) = <math>(Q_2 + Q_1) - 3\alpha - 8F_2 - 9F_4</math>            (6) 5) = <math>(-3/\sqrt{35})B_{2-2}</math>            (6) 6) = <math>(1/35)(17Q_2 + 47Q_1 + 6Q_0) - 3\alpha - 8F_2 - 9F_4</math>            (7) 5) = <math>(-2\sqrt{3}/\sqrt{35})B_{2-2}</math>            (7) 6) = <math>(2\sqrt{3}/35)(Q_2 - 3Q_1 + 2Q_0)</math>            (7) 7) = <math>(2/35)(9Q_2 + 22Q_1 + 4Q_0) + 4\alpha - 8F_2 - 9F_4</math>            (8) 5) = <math>(-\sqrt{2}/\sqrt{15})B_{2-2}</math>            (8) 6) = <math>(2/5\sqrt{42})(11Q_2 - 8Q_1 - 3Q_0)</math>            (8) 7) = <math>(4/5\sqrt{14})(-Q_2 + 2Q_1 - Q_0)</math>            (8) 8) = <math>(1/5)(6Q_2 + 3Q_1 + Q_0) - \alpha + 7F_2 - 84F_4</math>            (9) 5) = <math>(-2/\sqrt{15})B_{2-2}</math>            (9) 6) = <math>(2/5\sqrt{21})(-Q_2 + 4Q_1 - 3Q_0)</math>            (9) 7) = <math>(4/5\sqrt{7})(2Q_2 - Q_1 - Q_0)</math>            (9) 8) = <math>(\sqrt{2}/5)(-2Q_2 + 2Q_1 + Q_0)</math>            (9) 9) = <math>(2/5)(2Q_2 + 2Q_1 + Q_0) + 2\alpha + 7F_2 - 84F_4</math></p> <p>Singlet-triplet coupling matrix</p> <p>(5) 1) = <math>-2\alpha</math>            (6) 2) = <math>-2\alpha</math>            (7) 3) = <math>(4\sqrt{3}/\sqrt{5})\alpha</math>            (8) 3) = <math>(-42/\sqrt{5})\alpha</math>            (9) 4) = <math>(2/\sqrt{6})\alpha</math></p>	<p>Singlet-triplet coupling matrix</p> <p>(3) 1) = <math>-2\alpha</math>            (5) 2) = <math>(4\sqrt{3}/\sqrt{5})\alpha</math>            (6) 2) = <math>(-\sqrt{42}/\sqrt{5})\alpha</math></p> <p><math>\Gamma_4</math> Representation Singlet matrix</p> <p>(1) 1) = <math>(1/7)(3Q_2 + 8Q_1 + 3Q_0 - 3B_{2-2}) + 4F_2 + F_4</math>            (2) 1) = <math>(2\sqrt{3}/7)(Q_2 - 2Q_1 + Q_0 - B_{2-2})</math>            (2) 2) = <math>(2/7)(2Q_2 + 3Q_1 + 2Q_0 - 2B_{2-2}) - 3F_2 + 36F_4</math></p> <p>Triplet matrix</p> <p>(3) 3) = <math>(1/14)(11Q_2 + 8Q_1 + 9Q_0 + 9B_{2-2}) - 3\alpha - 8F_2 - 9F_4</math>            (4) 3) = <math>(i/\sqrt{28})(Q_2 - 2Q_1 + Q_0 + 3B_{2-2})</math>            (4) 4) = <math>(1/6)(5Q_2 + 4Q_1 + 3Q_0 - B_{2-2}) + \alpha - 8F_2 - 9F_4</math>            (5) 3) = <math>(1/7\sqrt{5})(-Q_2 + 5Q_1 - 4Q_0 + 3B_{2-2})</math>            (5) 4) = <math>(i/3\sqrt{35})(-Q_2 - 5Q_1 + 6Q_0 + 11B_{2-2})</math>            (5) 5) = <math>(1/105)(103Q_2 + 80Q_1 + 27Q_0 + 55B_{2-2}) + 4\alpha - 8F_2 - 9F_4</math>            (6) 3) = <math>(1/\sqrt{70})(3Q_2 - 3Q_0 + B_{2-2})</math>            (6) 4) = <math>(i/\sqrt{10})(Q_2 - Q_0 - B_{2-2})</math>            (6) 5) = <math>(1/5\sqrt{14})(2Q_2 - 2Q_0 + 5B_{2-2})</math>            (6) 6) = <math>(1/5)(2Q_2 + 6Q_1 + 3Q_0) - \alpha + 7F_2 - 84F_4</math></p> <p>Singlet-triplet coupling matrix</p> <p>(3) 1) = <math>-2\alpha</math>            (5) 2) = <math>(4\sqrt{3}/\sqrt{5})\alpha</math>            (6) 2) = <math>(-\sqrt{42}/\sqrt{5})\alpha</math></p> <p><math>\Gamma_5</math> Representation Singlet matrix</p> <p>(1) 1) = <math>Q_2 + Q_1 + 4F_2 + F_4</math>            (2) 1) = <math>(-1/\sqrt{7})B_{2-2}</math>            (2) 2) = <math>(1/7)(Q_2 + 7Q_1 + 6Q_0) + 4F_2 + F_4</math>            (3) 1) = <math>(-\sqrt{6}/7)B_{2-2}</math>            (3) 2) = <math>(\sqrt{6}/7)(Q_2 - Q_0)</math>            (3) 3) = <math>(1/7)(3Q_2 + 7Q_1 + Q_0) - 3F_2 + 36F_4</math></p> <p>Triplet matrix</p> <p>(4) 4) = <math>(1/4)(4Q_2 + Q_1 + 3Q_0) - 3\alpha - 8F_2 - 9F_4</math>            (5) 4) = <math>(3/2\sqrt{7})B_{2-2}</math>            (5) 5) = <math>(1/28)(16Q_2 + 31Q_1 + 9Q_0) - 3\alpha - 8F_2 - 9F_4</math>            (6) 4) = <math>(3/\sqrt{70})B_{2-2}</math>            (6) 5) = <math>(1/7\sqrt{10})(Q_2 - 2Q_1 + Q_0)</math>            (6) 6) = <math>(1/105)(80Q_2 + 64Q_1 + 66Q_0) + 4\alpha - 8F_2 - 9F_4</math>            (7) 4) = <math>(1/\sqrt{20})B_{2-2}</math>            (7) 5) = <math>(1/2\sqrt{35})(7Q_2 - 4Q_1 - 3Q_0)</math>            (7) 6) = <math>(4/5\sqrt{14})(-Q_1 + Q_0)</math>            (7) 7) = <math>(1/10)(10Q_2 + 7Q_1 + 3Q_0) - \alpha + 7F_2 - 84F_4</math>            (8) 4) = <math>(i\sqrt{3}/4)(Q_1 - Q_0)</math>            (8) 5) = <math>(i\sqrt{3}/2\sqrt{7})B_{2-2}</math>            (8) 6) = <math>(-11i/\sqrt{210})B_{2-2}</math>            (8) 7) = <math>(i\sqrt{3}/2\sqrt{5})B_{2-2}</math>            (8) 8) = <math>(1/4)(4Q_2 + 3Q_1 + Q_0) + \alpha - 8F_2 - 9F_4</math>            (9) 4) = <math>(-3i/2\sqrt{5})B_{2-2}</math>            (9) 5) = <math>(i/4\sqrt{35})(-4Q_2 + 11Q_1 - 7Q_0)</math>            (9) 6) = <math>(i/15\sqrt{14})(-13Q_2 + 34Q_1 - 21Q_0)</math>            (9) 7) = <math>(i/10)(3Q_2 - 4Q_1 + Q_0)</math>            (9) 8) = <math>(1/2\sqrt{15})B_{2-2}</math>            (9) 9) = <math>(1/60)(40Q_2 + 53Q_1 + 27Q_0) + \alpha - 8F_2 - 9F_4</math>            (10) 4) = <math>(-i/2\sqrt{5})B_{2-2}</math>            (10) 5) = <math>(i/2\sqrt{35})(Q_2 - 4Q_1 + 3Q_0)</math>            (10) 6) = <math>(4i/5\sqrt{14})(2Q_2 - Q_1 - Q_0)</math>            (10) 7) = <math>(3i/10)(2Q_2 - Q_1 - Q_0)</math>            (10) 8) = <math>(-\sqrt{3}/\sqrt{20})B_{2-2}</math>            (10) 9) = <math>(1/10)(5Q_2 - 4Q_1 - Q_0)</math>            (10) 10) = <math>(1/10)(10Q_2 + 7Q_1 + 3Q_0) + \alpha + 7F_2 - 84F_4</math></p> <p>Singlet-triplet coupling matrix</p> <p>(4) 1) = <math>-2\alpha</math>            (5) 2) = <math>-2\alpha</math>            (6) 3) = <math>(4\sqrt{3}/\sqrt{5})\alpha</math>            (7) 3) = <math>(-\sqrt{42}/\sqrt{5})\alpha</math></p>
---	--

TABLE VII  
 STRONG-FIELD BASIS FUNCTIONS

$\Gamma_1$ Representation Singlets	$\Gamma_4$ Representation Singlets
(1) = $aa[\alpha\beta]$	(1) = $[ac]^+[\alpha\beta]$
(2) = $bb[\alpha\beta]$	(2) = $[de]^+[\alpha\beta]$
(3) = $cc[\alpha\beta]$	Triplets
(4) = $(de)^+[\alpha\beta]$	(3) = $\{[ae](\alpha\beta)^+ -$
Triplets	$i[ad](\alpha\beta)\}/\sqrt{2}$
(5) = $[de](\alpha\beta)^+$	(4) = $\{[eb](\alpha\beta)^+ +$
(6) = $[bc](\alpha\beta)^+$	$i[db](\alpha\beta)\}/\sqrt{2}$
(7) = $\{[da](\alpha\beta)^+ -$	(5) = $\{[dc](\alpha\beta)^+ -$
$i[ea](\alpha\beta)\}/\sqrt{2}$	$i[ec](\alpha\beta)\}/\sqrt{2}$
(8) = $\{[db](\alpha\beta)^+ +$	(6) = $[ab](\alpha\beta)^+$
$i[eb](\alpha\beta)\}/\sqrt{2}$	$\Gamma_3$ Representation cosine-type
(9) = $\{[ce](\alpha\beta)^+ -$	functions
$i[cd](\alpha\beta)\}/\sqrt{2}$	Singlets
$\Gamma_2$ Representation Singlets	(1) = $[ad]^+[\alpha\beta]$
(1) = $[bc]^+[\alpha\beta]$	(2) = $[bd]^+[\alpha\beta]$
Triplets	(3) = $[ce]^+[\alpha\beta]$
(2) = $\{i[bd](\alpha\beta)^+ -$	Triplets
$[be](\alpha\beta)^+\}/\sqrt{2}$	(4) = $[ae](\alpha\beta)^+$
(3) = $\{[dc](\alpha\beta)^+ +$	(5) = $[be](\alpha\beta)^+$
$i[ec](\alpha\beta)\}/\sqrt{2}$	(6) = $[cd](\alpha\beta)^+$
(4) = $\{[ea](\alpha\beta)^+ +$	(7) = $[ab](\alpha\beta)^+$
$i[da](\alpha\beta)\}/\sqrt{2}$	(8) = $i[ac](\alpha\beta)$
$\Gamma_3$ Representation Singlets	(9) = $i[bc](\alpha\beta)$
(1) = $[ab]^+[\alpha\beta]$	(10) = $i[de](\alpha\beta)$
(2) = $(de)[\alpha\beta]$	$\Gamma_5$ Representation sine-type
Triplets	functions
(3) = $\{[da](\alpha\beta)^+ +$	Singlets
$i[ea](\alpha\beta)\}/\sqrt{2}$	(1) = $[ae]^+[\alpha\beta]$
(4) = $\{[db](\alpha\beta)^+ -$	(2) = $[be]^+[\alpha\beta]$
$i[eb](\alpha\beta)\}/\sqrt{2}$	(3) = $[cd]^+[\alpha\beta]$
(5) = $\{[ec](\alpha\beta)^+ +$	Triplets
$i[dc](\alpha\beta)\}/\sqrt{2}$	(4) = $[da](\alpha\beta)^+$
(6) = $[ac](\alpha\beta)^+$	(5) = $[bd](\alpha\beta)^+$
	(6) = $[ec](\alpha\beta)^+$
	(7) = $i[ab](\alpha\beta)$
	(8) = $[ca](\alpha\beta)^+$
	(9) = $[bc](\alpha\beta)^+$
	(10) = $[de](\alpha\beta)^+$

rather than by bending motions (in  $D_{4h}$  symmetry, the transitions in question are electronically forbidden and become observable only *via* odd vibrations). Whether the contributions due to bending really are negligible in comparison to those due to stretching also is open to question.

Finally, if peak 1 were due to the transition from the degenerate  $d_{xz}, d_{yz}$  orbitals, one would expect a splitting of this peak in the spectra of the complexes of lower symmetry, for example, in *trans*-Pt(NH<sub>3</sub>)<sub>2</sub>Cl<sub>2</sub>. Chatt, *et al.*,<sup>8</sup> rationalized the absence of any splitting by reasoning that the  $d_{x^2-y^2}$  orbital may be much more sensitive to the nature of the ligands than the  $d_{xz}$  and  $d_{yz}$  orbitals. In terms of the energy level assignment offered here, no splitting of the peak is expected since the transition is from the single  $d_{z^2}$  orbital.

II.—It may be asked whether the ordering of the d-levels found here really is characteristic of a square-planar ligand field or whether it is merely

a peculiar result of the additional assumptions (*e.g.*, the point-dipole model) used to carry through the calculations. This question can be answered only after a general characterization of a square-planar ligand field has been agreed upon. In the concluding section it is suggested that the relation  $4Dq + 7Dt = 0$  can reasonably be considered to qualify as such a characteristic. When this criterion is adopted, then the ordering of the d-levels proposed in this work is indeed a necessary general consequence without further detailed assumptions, as shown by the following reasoning.

Let the symbols  $\Delta A$ ,  $\Delta B$ ,  $\Delta E$  be used to denote the excitation energies corresponding to the transitions ( ${}^1A_1 \rightarrow {}^1A_2$ ), ( ${}^1A_1 \rightarrow {}^1B_1$ ), ( ${}^1A_1 \rightarrow {}^1E$ ), respectively. In the strong-field approximation, which is adequate for the present purpose, they are given by the differences between the corresponding diagonal elements of the matrix given in Table VIII. One finds from this table

$$\begin{aligned}\Delta A &= -35F_4 - 2B_{2-2} \\ \Delta B &= -4F_2 - 15F_4 + Q_0 - Q_2 - B_{2-2} \\ \Delta E &= -3F_2 - 20F_4 + Q_1 - Q_2 - B_{2-2}\end{aligned}$$

One now can substitute the relation  $F_2 = 14F_4$  quoted in Section 2 and express  $Q_0$ ,  $Q_1$ ,  $Q_2$ ,  $B_{2-2}$  by  $Dq$ ,  $Dt$ ,  $Ds$  according to Table IV. This yields the expressions

$$\begin{aligned}\Delta A &= -35F_4 - 10Dq \\ \Delta B &= -71F_4 - 4Ds - 5Dt \\ \Delta E &= -62F_4 - 10Dq - 3Ds + 5Dt\end{aligned}$$

which are general for tetragonal symmetry. The assumption of a square-planar field, if characterized by  $4Dq + 7Dt = 0$ , simplifies these formulas to

$$\Delta A = -35F_4 - 10Dq \quad (5)$$

$$\Delta B = -71F_4 - (20/7)Dq - 4Ds \quad (6)$$

$$\Delta E = -62F_4 - (90/7)Dq - 3Ds \quad (7)$$

Now  $F_4$  has the value 85 cm.<sup>-1</sup> as discussed in Section 2. Moreover we agree with Chatt, Gamlen, and Orgel that  $\Delta A = 25,500$  cm.<sup>-1</sup>, if we consider the case of [PtCl<sub>4</sub>]<sup>-2</sup> for concreteness. It follows then from eq. 5 that  $Dq = -2848$  cm.<sup>-1</sup> and hence

$$\Delta B = 2101 - 4Ds \quad (8)$$

$$\Delta E = 31347 - 3Ds \quad (9)$$

The next highest absorption in [PtCl<sub>4</sub>]<sup>-2</sup> lies at 30,200 cm.<sup>-1</sup>.

If this next band now is identified with  $\Delta E$ , then the value  $Ds = 382$  cm.<sup>-1</sup> is deduced from eq. 9 and there results  $\Delta B = 574$  cm.<sup>-1</sup>, implying that

TABLE VIII  
STRONG-FIELD MATRIX ELEMENTS

$\Gamma_1$ Representation Singlet matrix		Singlet-triplet coupling matrix	
(1) 1) = $2Q_0 + 4F_2 + 36F_4$		(5) 2) = $\sqrt{2}\alpha$	
(2) 1) = $4F_2 + 15F_4$		(6) 1) = $2i\alpha$	
(2) 2) = $2(Q_2 + B_{2-2}) + 4F_2 + 36F_4$		$\Gamma_4$ Representation Singlet matrix	
(3) 1) = $4F_2 + 15F_4$		(1) 1) = $Q_2 + Q_0 - B_{2-2} + 21F_4$	
(3) 2) = $35F_4$		(2) 1) = $2\sqrt{3}(F_2 - 5F_4)$	
(3) 3) = $2(Q_2 - B_{2-2}) + 4F_2 + 36F_4$		(2) 2) = $2Q_1 + F_2 + 16F_4$	
(4) 1) = $\sqrt{2}(F_2 + 30F_4)$		Triplet matrix	
(4) 2) = $\sqrt{2}(3F_2 + 20F_4)$		(3) 3) = $Q_1 + Q_0 - \alpha + F_2 - 54F_4$	
(4) 3) = $\sqrt{2}(3F_2 + 20F_4)$		(4) 3) = $3\sqrt{3}(-F_2 + 5F_4)$	
(4) 4) = $2Q_1 + 7F_2 + 56F_4$		(4) 4) = $Q_2 + Q_1 + B_{2-2} + \alpha - 5F_2 - 24F_4$	
Triplet matrix		(5) 3) = $3\sqrt{3}(F_2 - 5F_4)$	
(5) 5) = $2Q_2 - 5F_2 - 24F_4$		(5) 4) = $-3F_2 + 15F_4 + 2\alpha$	
(6) 5) = $6F_2 - 30F_4$		(5) 5) = $Q_2 + Q_1 - B_{2-2} + \alpha - 5F_2 - 24F_4$	
(6) 6) = $2Q_1 + 4F_2 - 69F_4$		(6) 3) = $-i\sqrt{2}\alpha$	
(7) 5) = $-i\sqrt{6}\alpha$		(6) 4) = $-i\sqrt{6}\alpha$	
(7) 7) = $Q_1 + Q_0 + F_2 - 54F_4 + \alpha$		(6) 6) = $Q_2 + Q_0 + B_{2-2} - 8F_2 - 9F_4$	
(8) 5) = $-i\sqrt{2}\alpha$		Singlet-triplet coupling matrix	
(8) 6) = $i\sqrt{2}\alpha$		(3) 1) = $2\alpha$	
(8) 7) = $3\sqrt{3}(-F_2 + 5F_4)$		(3) 2) = $-\sqrt{6}\alpha$	
(8) 8) = $Q_2 + Q_1 + B_{2-2} - \alpha - 5F_2 - 24F_4$		(4) 2) = $-2\alpha$	
(9) 5) = $i\sqrt{2}\alpha$		(5) 1) = $\sqrt{6}\alpha$	
(9) 6) = $-i\sqrt{2}\alpha$		(5) 2) = $-\sqrt{2}\alpha$	
(9) 7) = $3\sqrt{3}(F_2 - 5F_4)$		(6) 1) = $-2i\alpha$	
(9) 8) = $2\alpha - 3F_2 + 15F_4$		$\Gamma_5$ Representation Singlet matrix	
(9) 9) = $Q_2 + Q_1 - B_{2-2} - \alpha - 5F_2 - 24F_4$		(1) 1) = $Q_1 + Q_0 + 3F_2 + 6F_4$	
Singlet-triplet coupling matrix		(2) 1) = $\sqrt{3}(F_2 - 5F_4)$	
(5) 4) = $-2i\alpha$		(2) 2) = $Q_2 + Q_1 + B_{2-2} + F_2 + 16F_4$	
(6) 2) = $i\sqrt{8}\alpha$		(3) 1) = $\sqrt{3}(-F_2 + 5F_4)$	
(6) 3) = $i\sqrt{8}\alpha$		(3) 2) = $3F_2 - 15F_4$	
(7) 1) = $2\sqrt{3}\alpha$		(3) 3) = $Q_2 + Q_1 - B_{2-2} + F_2 + 16F_4$	
(7) 4) = $-\sqrt{6}\alpha$		Triplet matrix	
(8) 2) = $-2\alpha$		(4) 4) = $Q_1 + Q_0 + F_2 - 54F_4$	
(8) 4) = $\sqrt{2}\alpha$		(5) 4) = $3\sqrt{3}(F_2 - 5F_4)$	
(9) 3) = $2\alpha$		(5) 5) = $Q_2 + Q_1 + B_{2-2} - 5F_2 - 24F_4$	
(9) 4) = $-\sqrt{2}\alpha$		(6) 4) = $-3\sqrt{3}(F_2 - 5F_4)$	
$\Gamma_2$ Representation Singlet matrix		(6) 5) = $-3F_2 + 15F_4$	
(1) 1) = $2Q_2 + 4F_2 + F_4$		(6) 6) = $Q_2 + Q_1 - B_{2-2} - 5F_2 - 24F_4$	
Triplet matrix		(7) 4) = $-i\alpha$	
(2) 2) = $Q_2 + Q_1 + B_{2-2} - \alpha - 5F_2 - 24F_4$		(7) 5) = $i\sqrt{3}\alpha$	
(3) 2) = $-2\alpha - 3F_2 + 15F_4$		(7) 7) = $Q_2 + Q_0 + B_{2-2} - 8F_2 - 9F_4$	
(3) 3) = $Q_2 + Q_1 - B_{2-2} - \alpha - 5F_2 - 24F_4$		(8) 4) = $i\alpha$	
(4) 2) = $3\sqrt{3}(F_2 - 5F_4)$		(8) 6) = $i\sqrt{3}\alpha$	
(4) 3) = $-3\sqrt{3}(F_2 - 5F_4)$		(8) 7) = $-2\alpha$	
(4) 4) = $Q_1 + Q_0 + \alpha + F_2 - 54F_4$		(8) 8) = $Q_2 + Q_0 - B_{2-2} - 8F_2 - 9F_4$	
Singlet-triplet coupling matrix		(9) 5) = $i\alpha$	
(2) 1) = $-\sqrt{2}\alpha$		(9) 6) = $-i\alpha$	
(3) 1) = $-\sqrt{2}\alpha$		(9) 9) = $2Q_2 + 4F_2 - 69F_4$	
$\Gamma_3$ Representation Singlet matrix		(10) 4) = $i\sqrt{3}\alpha$	
(1) 1) = $Q_2 + Q_0 + B_{2-2} + 21F_4$		(10) 5) = $-i\alpha$	
(2) 1) = $2\sqrt{3}(F_2 - 5F_4)$		(10) 6) = $i\alpha$	
(2) 2) = $2Q_1 + F_2 + 16F_4$		(10) 9) = $-6F_2 + 30F_4$	
Triplet matrix		(10) 10) = $2Q_1 - 5F_2 - 24F_4$	
(3) 3) = $Q_1 + Q_0 - \alpha + F_2 - 54F_4$		Singlet-triplet coupling matrix	
(4) 3) = $3\sqrt{3}(-F_2 + 5F_4)$		(4) 1) = $i\alpha$	
(4) 4) = $Q_2 + Q_1 + B_{2-2} + \alpha - 5F_2 - 24F_4$		(5) 2) = $-i\alpha$	
(5) 3) = $3\sqrt{3}(-F_2 + 5F_4)$		(5) 3) = $2i\alpha$	
(5) 4) = $-2\alpha + 3F_2 - 15F_4$		(6) 2) = $2i\alpha$	
(5) 5) = $Q_2 + Q_1 - B_{2-2} + \alpha - 5F_2 - 24F_4$		(6) 3) = $-i\alpha$	
(6) 3) = $-i\sqrt{2}\alpha$		(7) 1) = $-\alpha$	
(6) 5) = $-i\sqrt{6}\alpha$		(7) 2) = $\sqrt{3}\alpha$	
(6) 6) = $Q_2 + Q_0 - B_{2-2} - 8F_2 - 9F_4$		(8) 1) = $\alpha$	
Singlet-triplet coupling matrix		(8) 3) = $\sqrt{3}\alpha$	
(3) 1) = $-\sqrt{2}\alpha$		(9) 2) = $-\alpha$	
(3) 2) = $\sqrt{6}\alpha$		(9) 3) = $\alpha$	
(4) 1) = $\sqrt{6}\alpha$		(10) 1) = $\sqrt{3}\alpha$	
(4) 2) = $-\sqrt{2}\alpha$		(10) 2) = $-\alpha$	
		(10) 3) = $\alpha$	

${}^1B_1$  is practically identical with the ground state, *i.e.*, that the orbitals  $5d_{z^2}$  and  $5d_{(x^2-y^2)}$  are almost degenerate. Hence the ligand field would be very close to having octahedral symmetry in complete contradiction to the initial assumption of a square-planar situation. This choice therefore is impossible.

If, on the other hand, the  $30,200\text{ cm.}^{-1}$  band is identified with  $\Delta B$ , as in the main body of this investigation, then eq. 8 yields  $D_s = -7025\text{ cm.}^{-1}$ , one obtains  $\Delta E = 52,422\text{ cm.}^{-1}$ , and there arise no contradictions.

### Conclusion

The good agreement with spectral observations appears to indicate that the potential given in eq. 3, modified for the dipole model, describes well the actual potential responsible for the splitting of the  $d^8$ -configuration. It is obtained by two assumptions, in addition to that of tetragonal symmetry: (1) the assumption of the point-dipole model; (2) the assumption of a square-planar physical situation, *i.e.*, the absence of point dipoles on the  $z$ -axis.

The first of these really is without consequence, it merely provides certain (convenient, but fictitious) pictures for the expansion of the potential in spherical harmonics. In reality, this potential does of course not arise from actual point dipoles.

The second approximation has, however, physical content, since it results in the *three* tetragonal parameters  $Dq$ ,  $D_s$ ,  $Dt$  being expressed in terms of *two* parameters  $B_2$ ,  $B_4$  of eq. 4 by the relations

$$\begin{aligned} Dq &= (1/6)B_4 \\ D_s &= (-2/7)B_2 \\ Dt &= (-2/21)B_4 \end{aligned}$$

One also can say that, for the point-dipole model, the case of square-planar *physics*<sup>16</sup> is characterized by the constraint

$$4Dq + 7Dt = 0$$

within the tetragonal *symmetry*.

Since this constraint appears to be compatible with the potential acting in the Pt-complexes, the conjecture seems to be justified that this relation possibly might be considered as a general characterization of what one has to mean by a square-planar ligand-field. In any case these considerations indicate that an appropriate definition of the square-planar situation within tetragonal symmetry, but without reference to the point-dipole

or point-charge model, would seem to deserve analysis.

### Appendix. Weak-Field and Strong-Field Basis Functions and Matrix Elements

**Definitions and Notation.**—(1) Tables III–VIII present the weak-field and the strong-field basis functions for the  $d^2$  configuration in  $D_4$  symmetry, and the corresponding matrix elements of the type defined by eq. 2 for the  $d^8$  configuration. The matrix elements of the  $d^2$  configuration are obtained from those of the  $d^8$  configuration by changing the signs of the quantities  $\alpha$ ,  $B_2$ ,  $B_4$ , but leaving the signs of  $F_2$ ,  $F_4$  unchanged.

The basis functions within one representation are simply identified by numbers, *viz.*, (1), (2), etc. The corresponding matrix elements  $H'_{ij}$  of eq. 2 are simply denoted by the symbols (1|2), (1|3), (2|3), etc.

Only the non-vanishing matrix elements are listed. Matrix elements which are not listed are zero. Also, of the two matrix elements,  $(i|j)$  and  $(j|i)$ , only one is listed; the other can be obtained from the fact that the matrix  $H'$  is hermitean, so that  $(j|i) = (i|j)^*$ .

(2) The weak-field functions are given in Table V. They are expressed in terms of the basis functions of the  $L$ - $S$  coupling scheme. The familiar notation  ${}^1L_J(M_J)$ ,  ${}^3L_J(M_J)$  is used, where  $L = 0, 1, 2, 3, 4$  is expressed as  $L = S, P, D, F, G$ , and  $J, M_J$  denote the quantum numbers of absolute value and  $z$ -component of the total angular momentum.

*Attention should be paid to the fact that the phases of these functions are defined in exact agreement with Condon and Shortley.<sup>8</sup>*

(3) The strong-field functions are given in Table VII. They are expressed directly in terms of the one-electron functions, *viz.*, the spin functions  $\alpha$ ,  $\beta$ , and the symmetry-adapted  $5d$ -orbitals given in Table III.

Moreover the following abbreviations are used in Table VII for any two functions  $f(x)$  and  $g(x)$

$$\begin{aligned} [fg] &= [f(x)g(y) - g(x)f(y)]/\sqrt{2} \\ [fg]^+ &= [f(x)g(y) + g(x)f(y)]/\sqrt{2} \\ (fg) &= [f(x)f(y) - g(x)g(y)]/\sqrt{2} \\ (fg)^+ &= [f(x)f(y) + g(x)g(y)]/\sqrt{2} \end{aligned}$$

(4) The weak-field matrix elements are given in Table VI; the strong-field matrix elements are given in Table VIII. All matrix elements are expressed in terms of the parameters

$F_2, F_4 =$  Slater-Condon electron-interaction parameters

$\alpha = 1/2\xi =$  Condon-Shortley spin-orbit parameters

$$\left. \begin{aligned} Q_m &= \langle l, m | V(D_{4h}) | l, m \rangle = \\ &\quad \langle l, -m | V(D_{4h}) | l, -m \rangle \\ B_{m-m} &= \langle l, m | V(D_{4h}) | l, -m \rangle = \\ &\quad \langle l, -m | V(D_{4h}) | l, +m \rangle \end{aligned} \right\} \begin{array}{l} \text{ligand-field} \\ \text{integrals.} \end{array}$$

The ligand-field integrals can be expressed in terms of 3 parameters,  $Dq$ ,  $Dt$ ,  $D_s$ , for a general tetragonal potential, as discussed by Liehr<sup>9</sup> and Moffitt and Ballhausen.<sup>2</sup> The expressions are given in column two of Table IV. In the case of the square-planar point-dipole model, they can be expressed in terms of the two integrals  $B_2$ ,  $B_4$ , defined in eq. 4. These expressions are given in column three of Table IV.

(16) It is incorrect to speak of square-planar *symmetry*.